



Ecografia B Scan vs OCT

Nicola Rosa

**Direttore Cattedra di Malattie dell'Apparato Visivo
Università di Salerno**

The background of the slide is a dark blue color. It features several sets of concentric circles in a lighter blue shade, arranged in a pattern that resembles a Venn diagram or a series of overlapping ripples. The circles are centered around the text.

L'OCT ha diminuito le
indicazioni dell'ecografia?

The background of the slide features a dark blue field with several sets of concentric, light blue circles. These circles are arranged in a pattern that overlaps, creating a sense of depth and movement. The circles are centered around the text, with some appearing larger and more prominent than others.

A Scan

B Scan



Ecografia

OCT

INDICAZIONI DELL' OCT

Mezzi diottrici trasparenti

INDICAZIONI DELL' ECOGRAFIA

Mezzi diottrici opachi

Patologie orbitarie

The background of the slide is a dark blue color. It features a pattern of several overlapping, concentric circles in a lighter shade of blue. These circles are centered at different points, creating a complex, layered geometric design. The text is centered horizontally and vertically over this pattern.

Ecografia

Oftalmoscopia

MEZZI DIOTTRICI TRASPARENTI

Neoformazioni

Distacco di retina

Lacerazioni

Maculopatie

MEZZI DIOTTRICI OPACHI

Neoformazioni

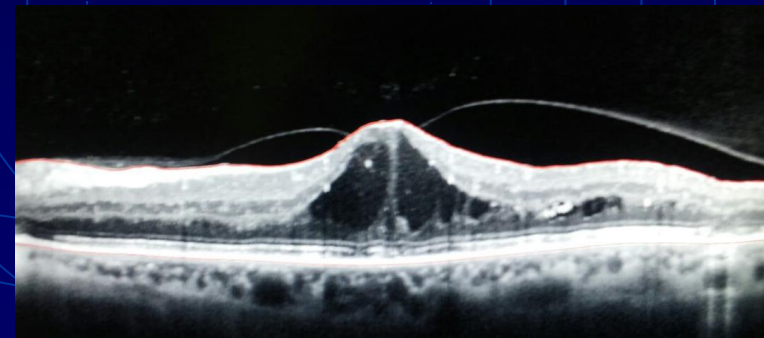
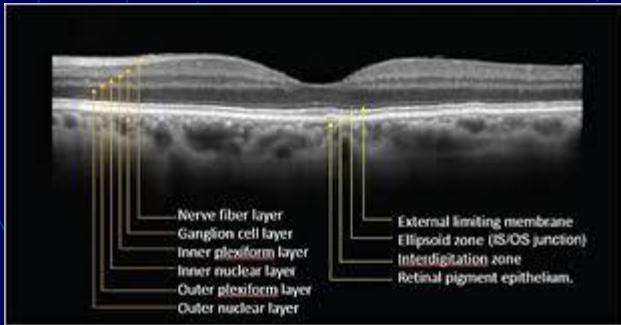
Distacco di retina

Lacerazioni

Maculopatie

RISOLUZIONE

OCT: 12 micron

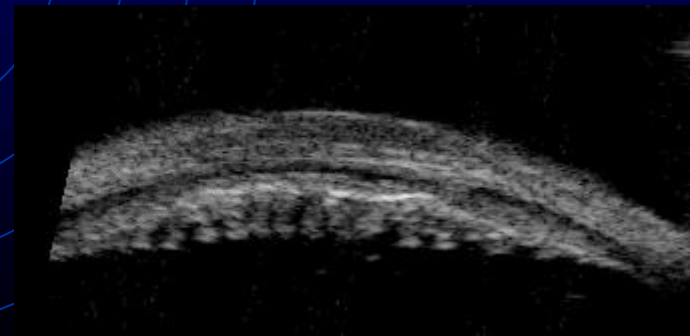


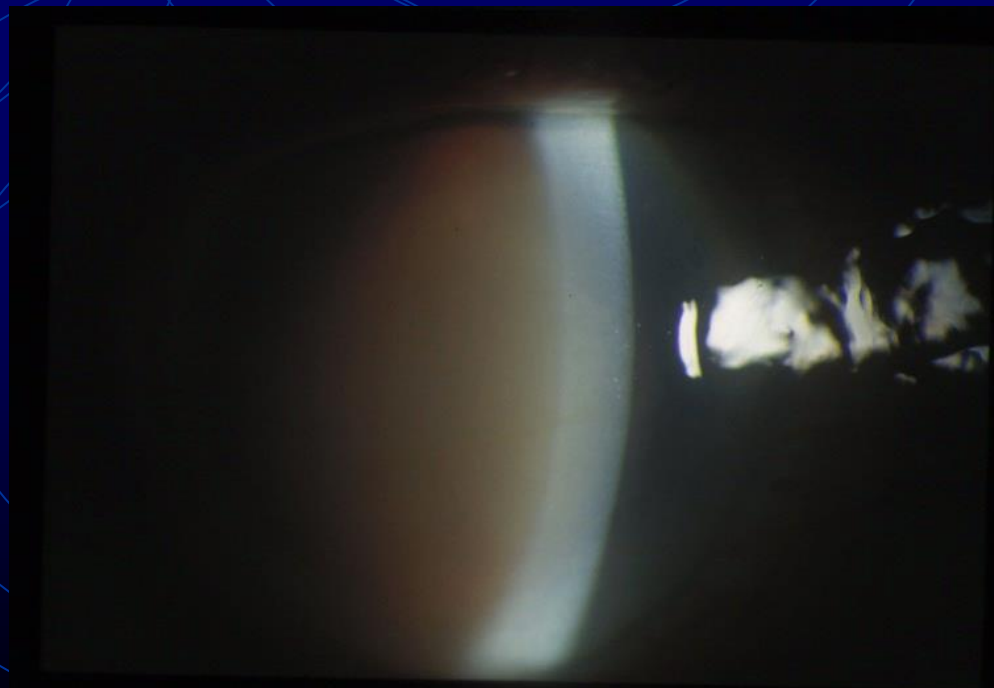
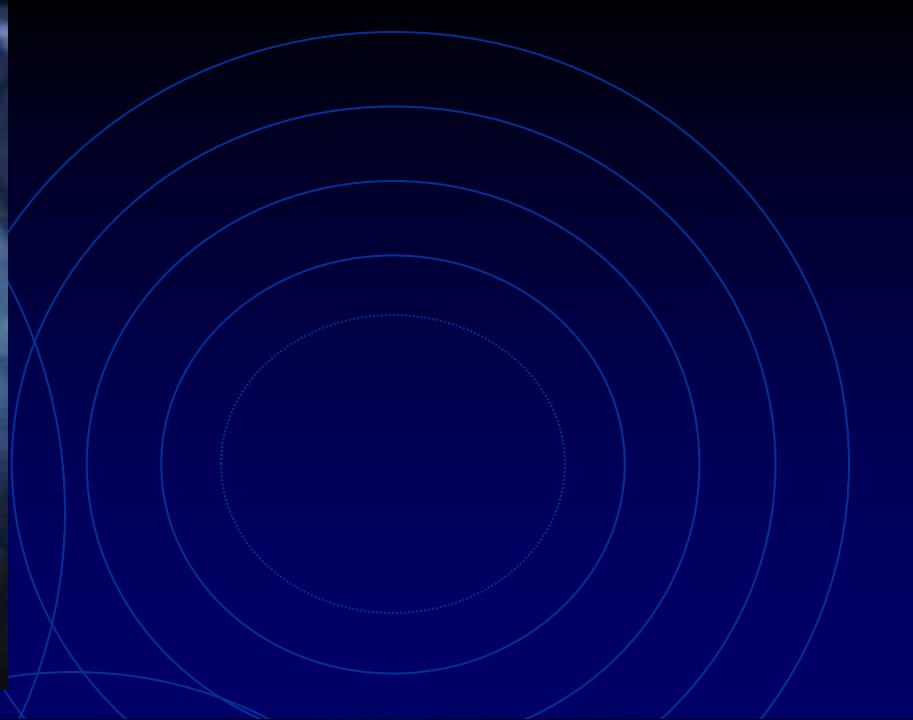
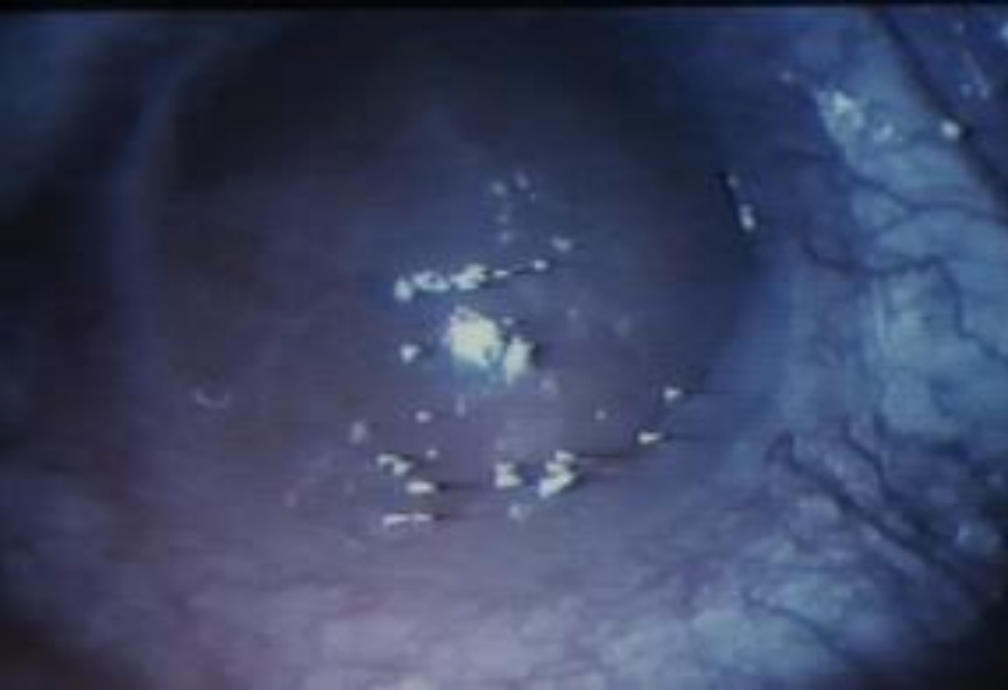
Eco:

150 micron



50 micron





MEZZI DIOTTRICI OPACHI

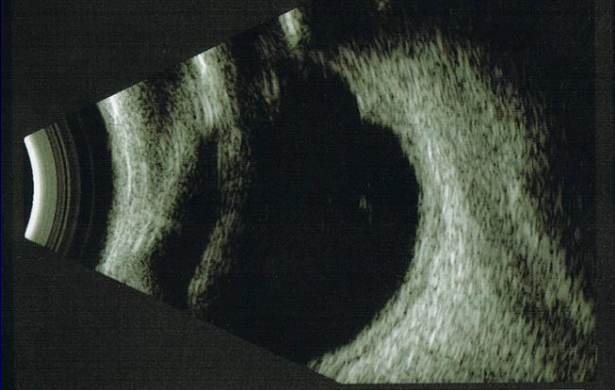
Neoformazioni

Distacco di retina

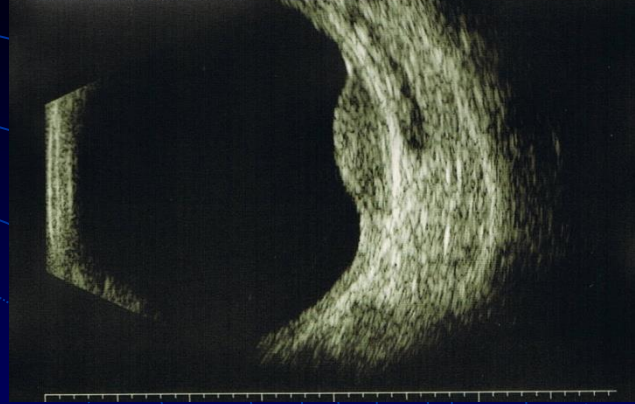
Lacerazioni

Maculopatie

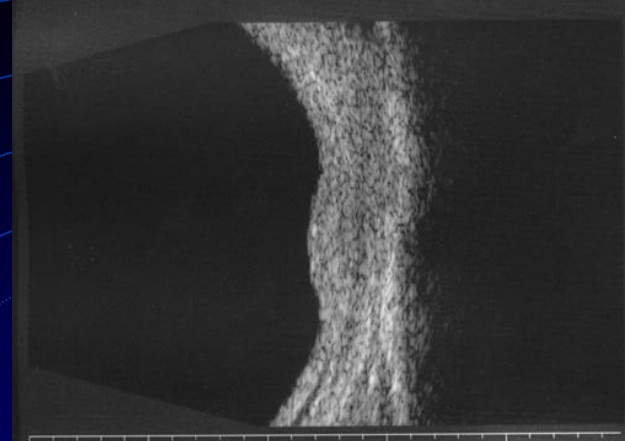
LEFT <5445L4 > G= 84dB DYN= 50dB TGC= 0dB 18/18
Quantel Medical CineScan S V:5.2.03



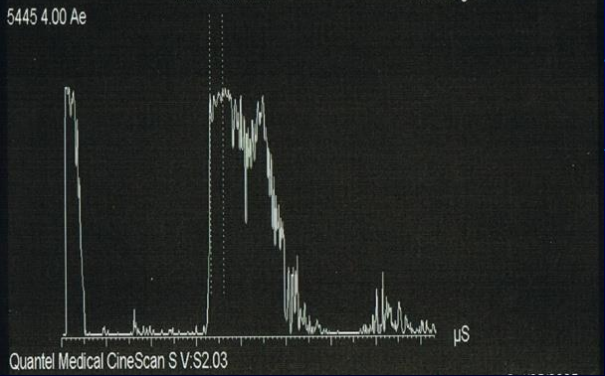
LEFT <7976T8E > G= 91dB DYN= 60dB TGC= 0dB 39/39
Quantel Medical CineScan S V:5.06



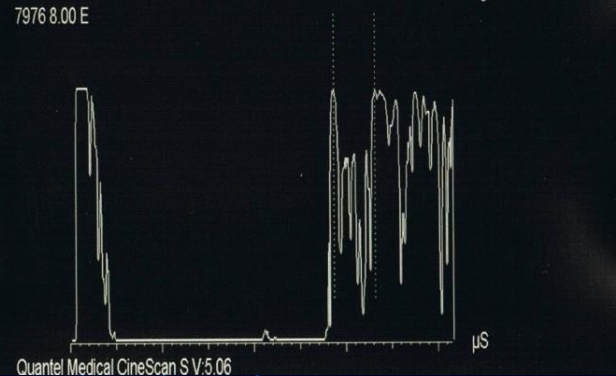
LEFT <4102T3EA > G= 97dB DYN= 50dB TGC=-10dB 39/39



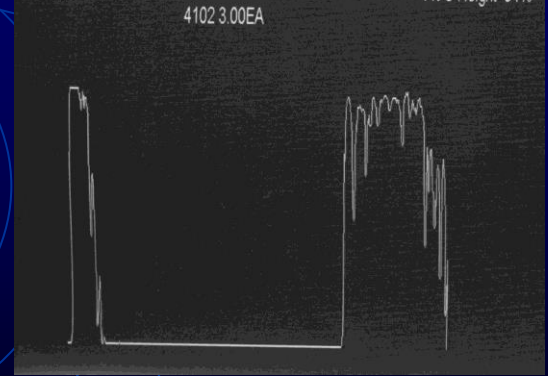
Bio2 Q1 K A1 LEFT #1 EYE T= 73.0dB
Velocity (m/s) : 1550 Distance= 2.17mm
ATT=0.00dB/mm
Quant-I=96%
AVG Height=94%



Bio2 Q-I K LEFT #3 EYE T= 72.9dB
Velocity (m/s) : 1550 Distance= 3.37mm
Quant-I=75%
AVG Height=65%



Bio2 Q-I K LEFT #1 EYE T= 73.8dB
Velocity (m/s) : 1550 Distance= 2.94mm
Quant-I=95%
AVG Height=91%



MEZZI DIOTTRICI OPACHI

Neoformazioni

Distacco di retina

Lacerazioni

Maculopatie

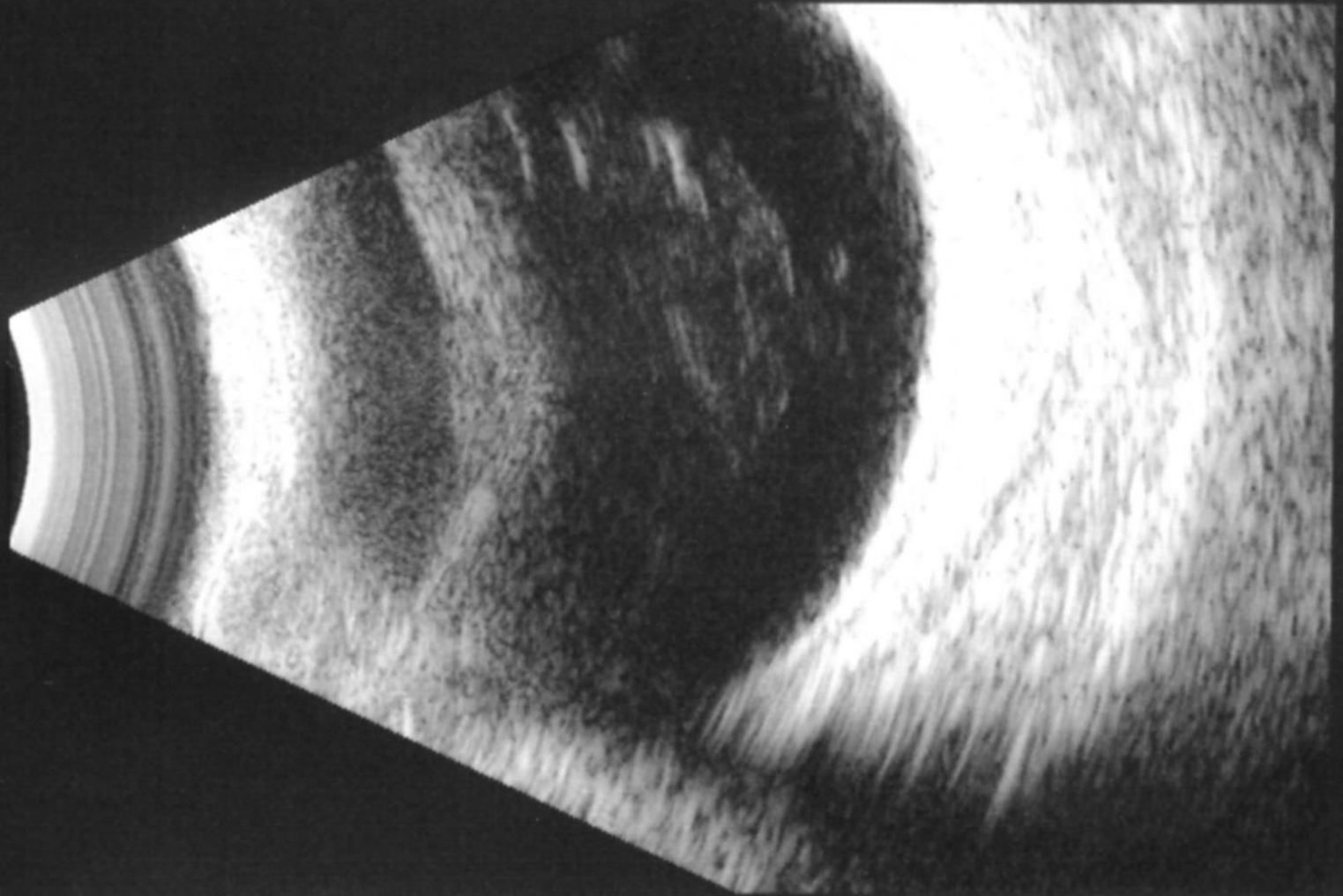
The background features a dark blue field with several overlapping, concentric circles in a lighter blue shade. The circles are arranged in a way that they partially overlap each other, creating a complex geometric pattern. The text is centered horizontally and stacked vertically.

PRE OPERATORIO

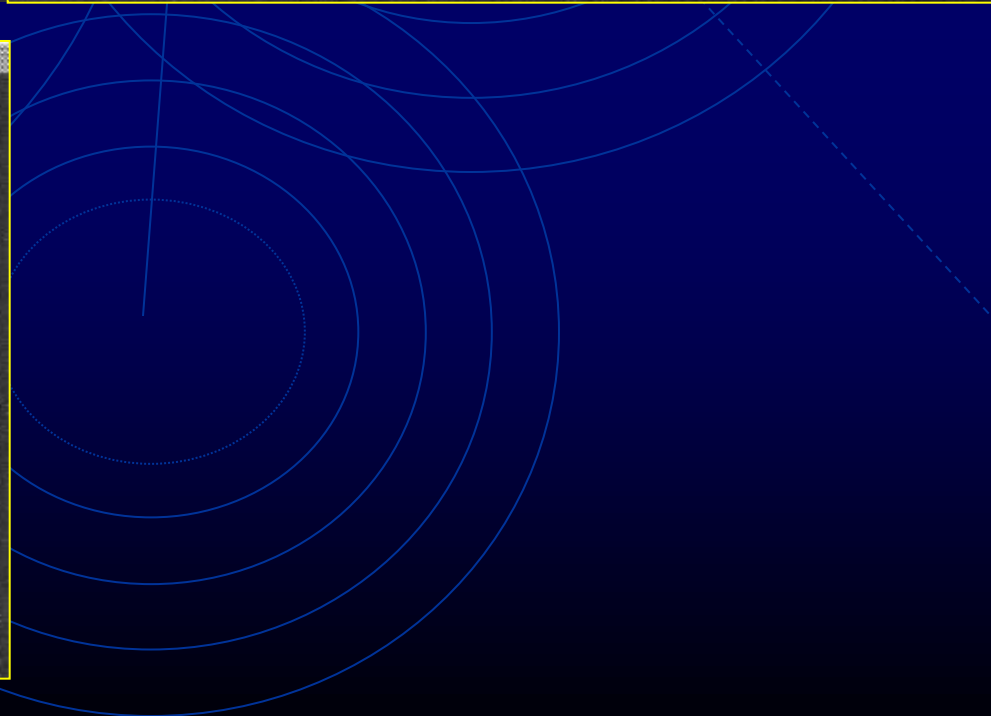
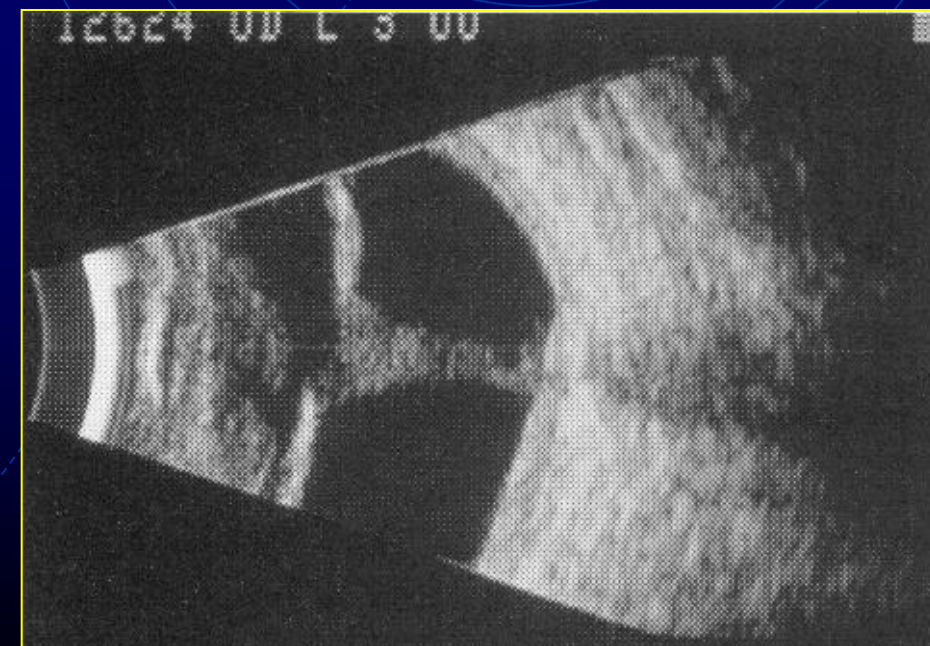
DIAGNOSTICARE

STADIARE

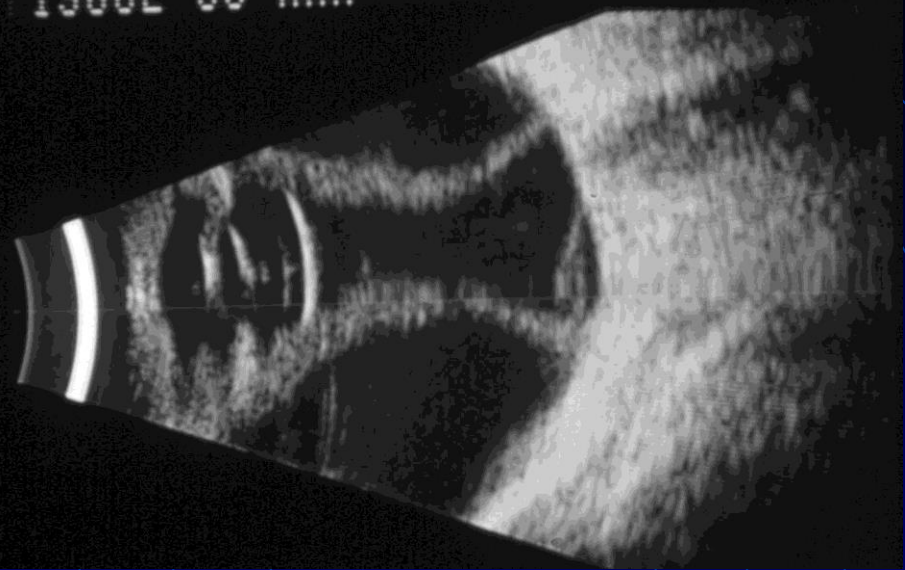
LEFT <5399T12E > G= 103dB DYN= 50dB TGC= 0dB 18/18
Quantel Medical CineScan S V:S2.03



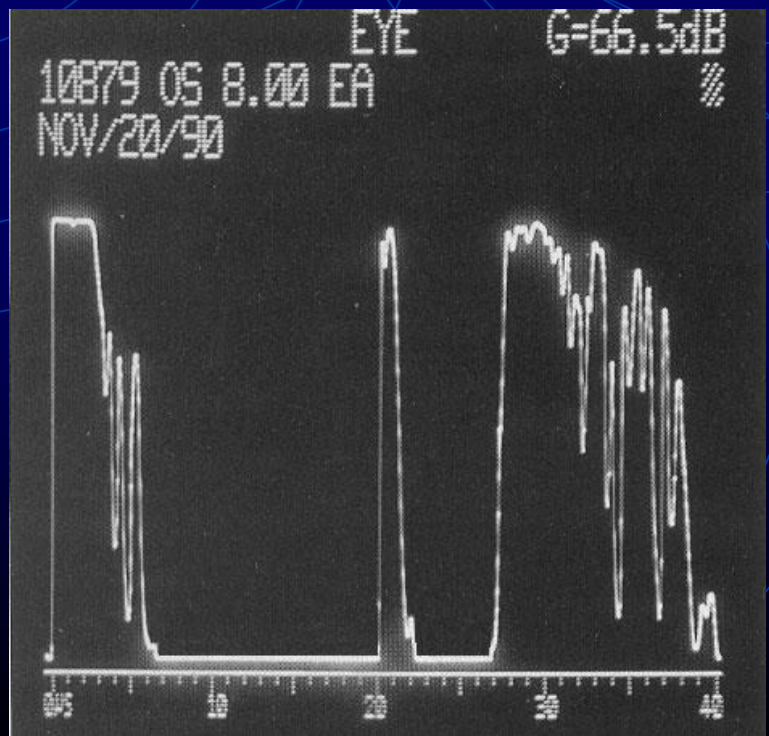
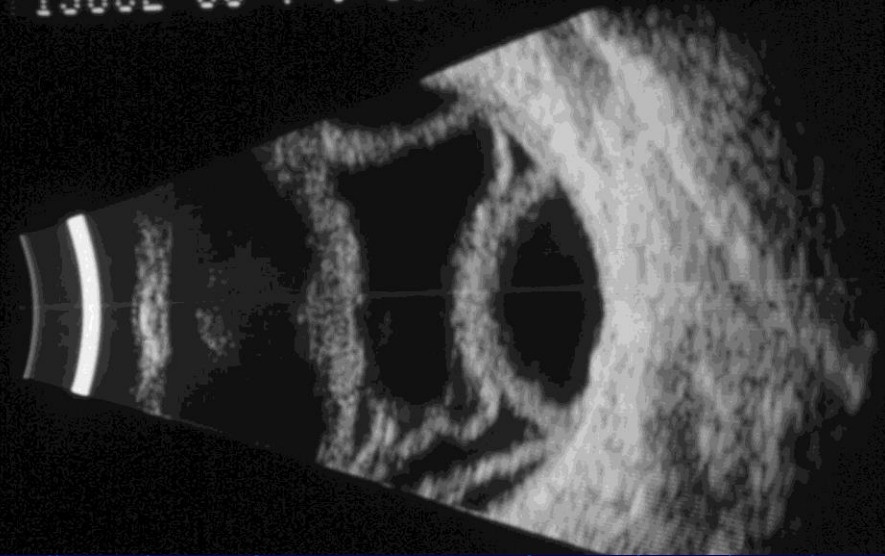
LEFT <3144L9 > G= 86dB DYN= 50dB TGC= 0dB 18/18
Quantel Medical CineScan S V:S2.03

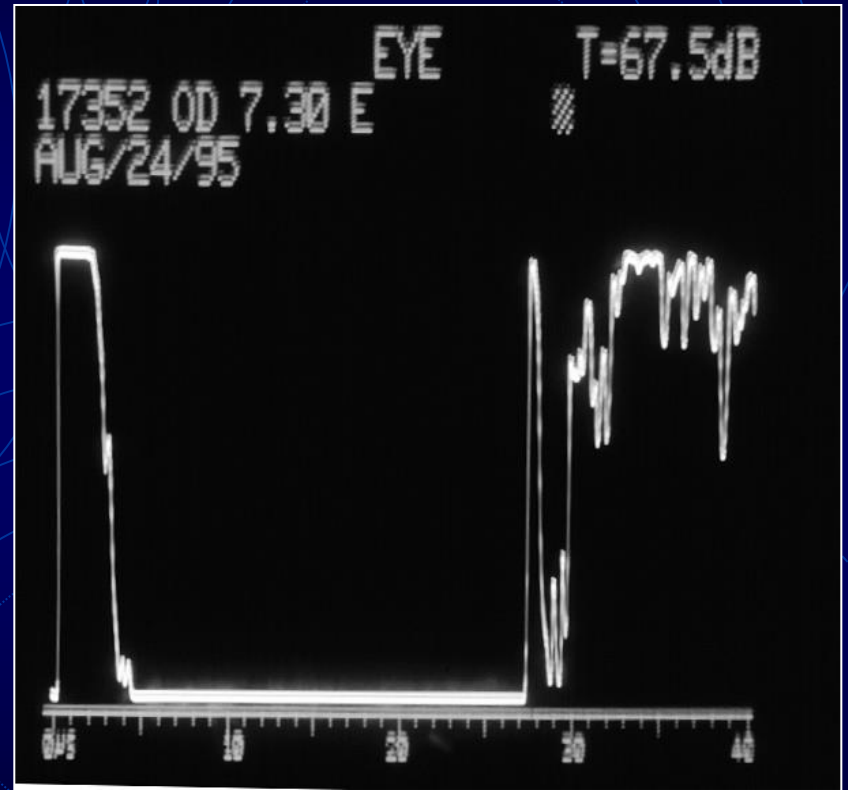


13882 OS HAX



13882 OS T 9 00 E





MEZZI DIOTTRICI OPACHI

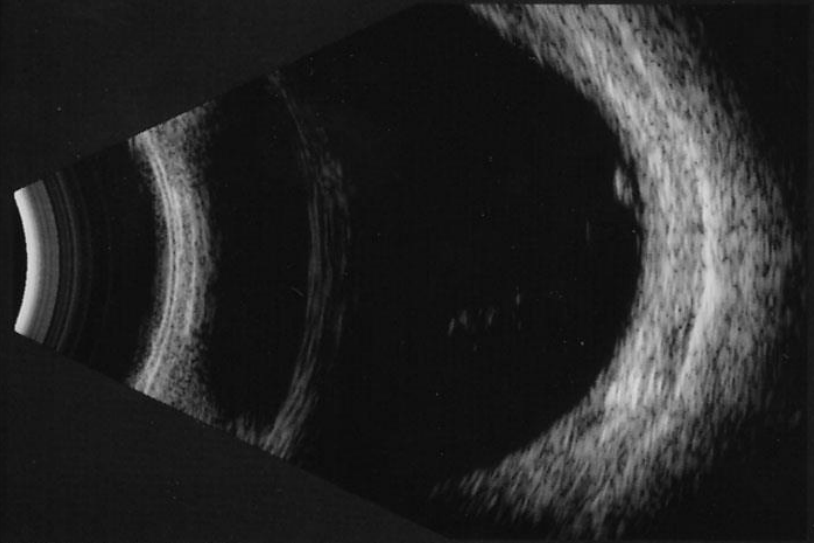
Neoformazioni

Distacco di retina

Lacerazioni

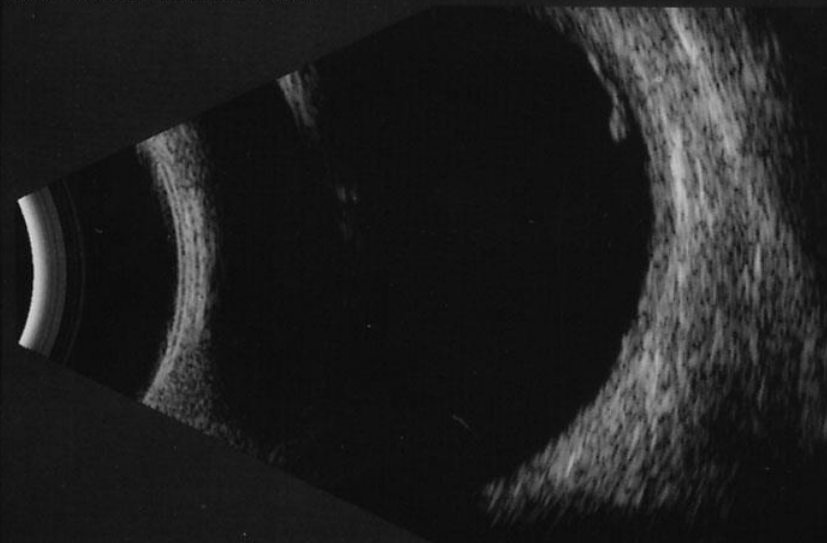
Maculopatie

LEFT <3815 T11 > G= 80dB DYN= 50dB TGC= 0dB 18/18
Quantel Medical CineScan S V:S2.03



July/10/2003

LEFT <3815L11 > G= 75dB DYN= 50dB TGC= 0dB 18/18
Quantel Medical CineScan S V:S2.03



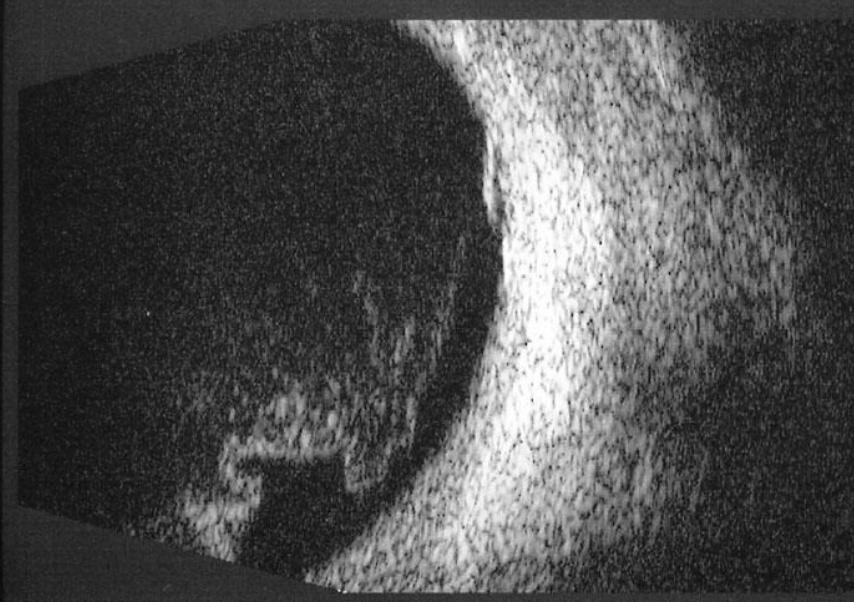
July/10/2003

LEFT <4170L2 > G= 99dB DYN= 50dB TGC=-10dB 36/39



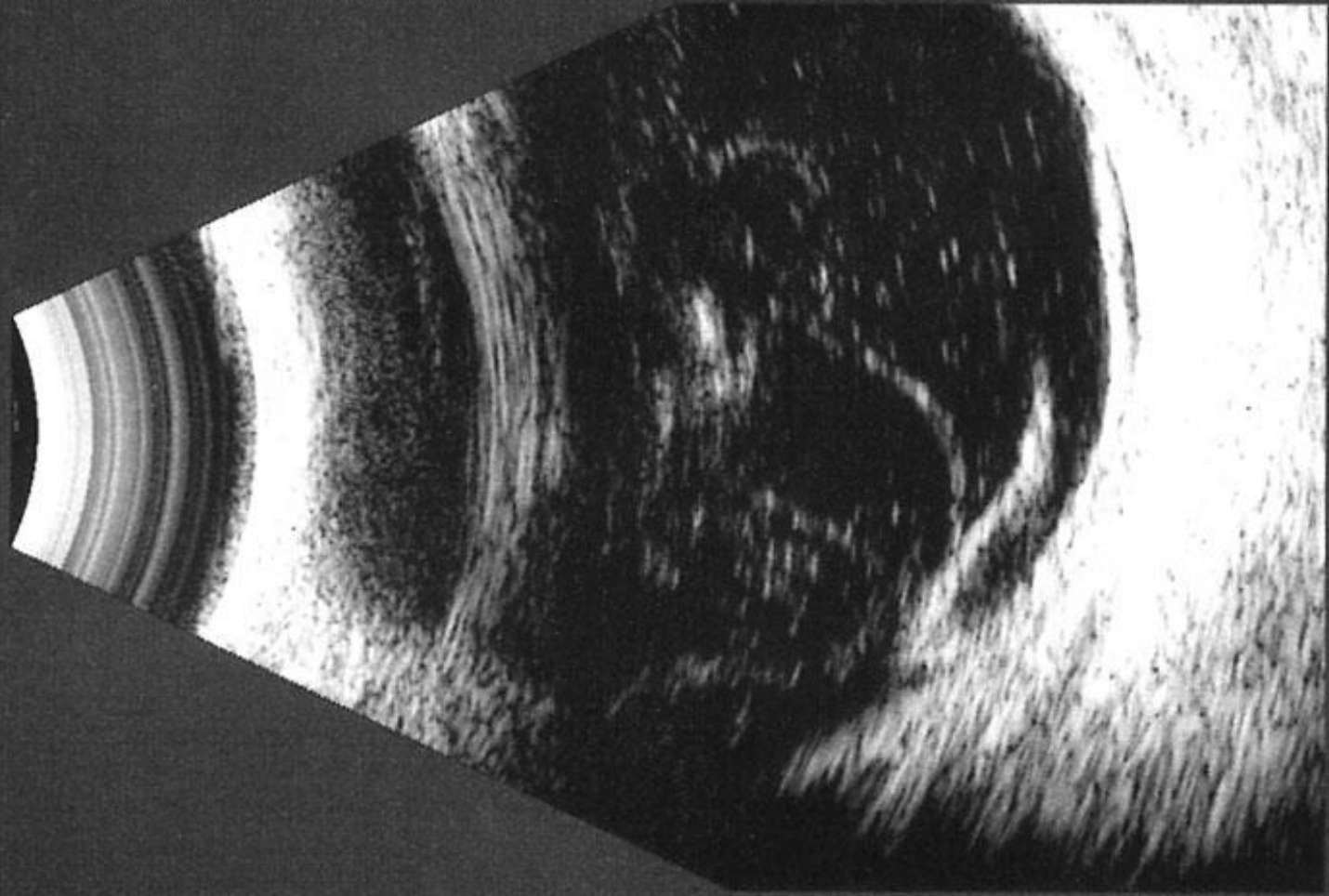
Jan/14/2004 10 MHz

LEFT <4170L2 > G= 105dB DYN= 50dB TGC=-10dB 34/39



Jan/14/2004 20 MHz

LEFT <2526T2EA > G= 91dB DYN= 50dB TGC= 0dB 18/18
Quantel Medical CineScan S V:S2.03

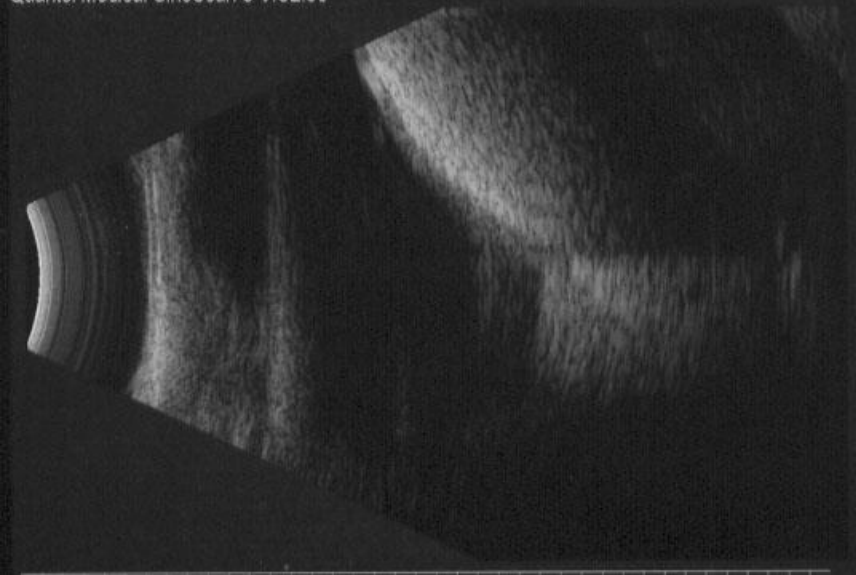


Feb/03/2003



POST INTERVENTO

LEFT <2390L7 > G= 83dB DYN= 50dB TGC= 0dB 18/18
Quantel Medical CineScan S V:S2.03

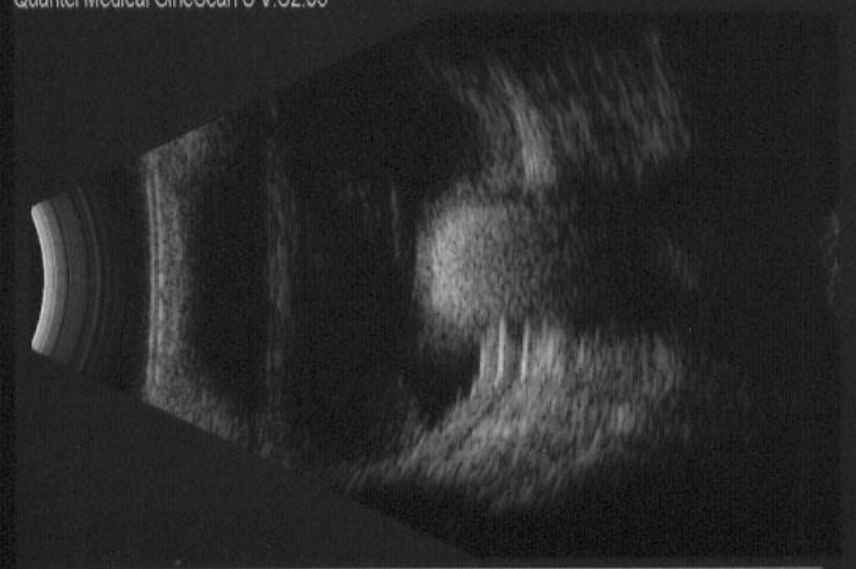


RIGHT <3150L9 > G= 77dB DYN= 50dB TGC= 0dB 18/18
Quantel Medical CineScan S V:S2.03

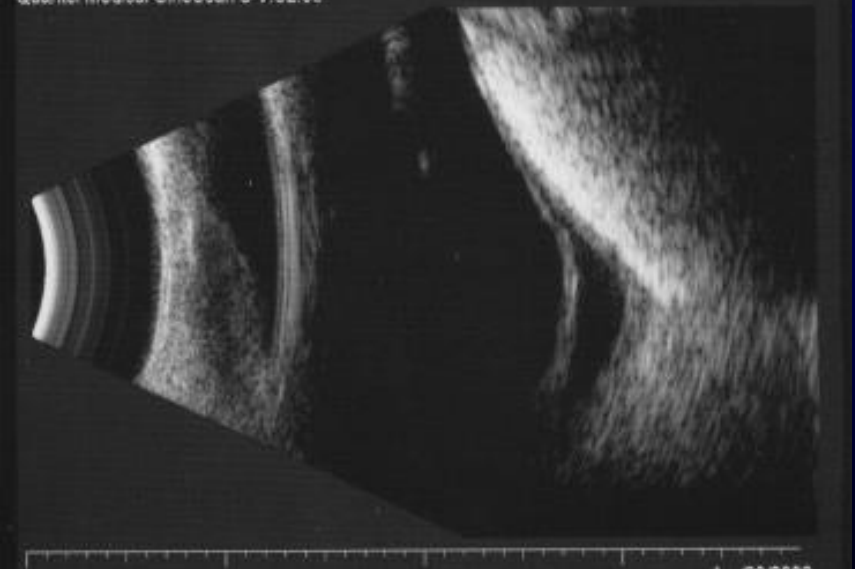


POST OPERATORIO

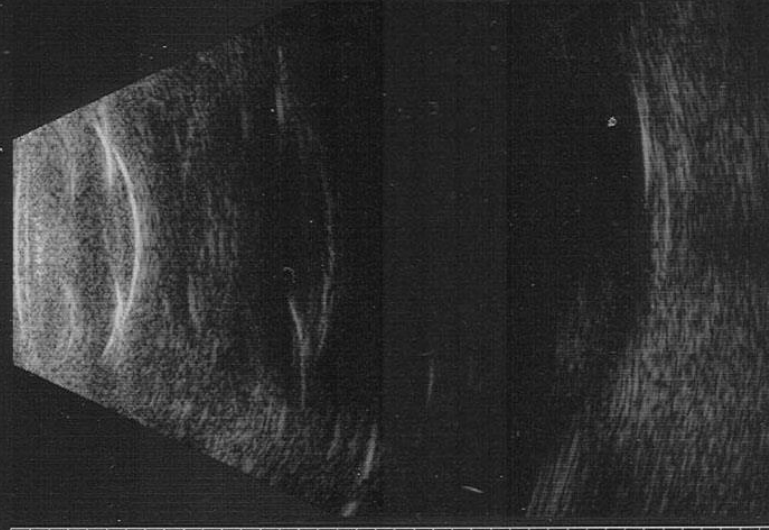
LEFT <2390T 7E > G= 82dB DYN= 50dB TGC= 0dB 18/18
Quantel Medical CineScan S V:S2.03



RIGHT <3150L103 > G= 80dB DYN= 50dB TGC= 0dB 18/18
Quantel Medical CineScan S V:S2.03

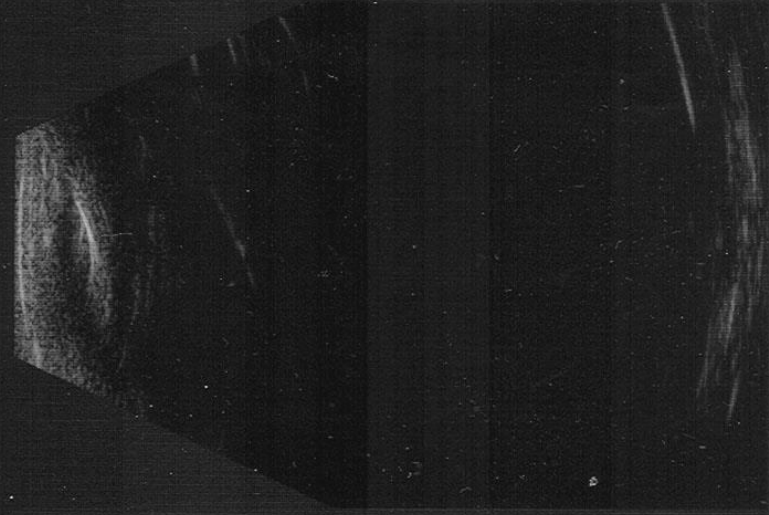


RIGHT <7017VAX > G= 105dB DYN= 60dB TGC= 0dB 39/39
Quantel Medical CineScan S V:5.06



Oct/20/2008 10 MHz

RIGHT <7017L9 > G= 86dB DYN= 60dB TGC= 0dB 39/39
Quantel Medical CineScan S V:5.06



Oct/20/2008 10 MHz

MEZZI DIOTTRICI OPACHI

Neoformazioni

Distacco di retina

Lacerazioni

Maculopatie

Macula study with standardized echography

G. Cennamo¹, N. Rosa¹, G. Iaccarino², A. La Rana¹
and A. Pasquariello¹

Department of Ophthalmology¹, University of Naples - Federico II, and
Eye Department², II University of Naples, Italy

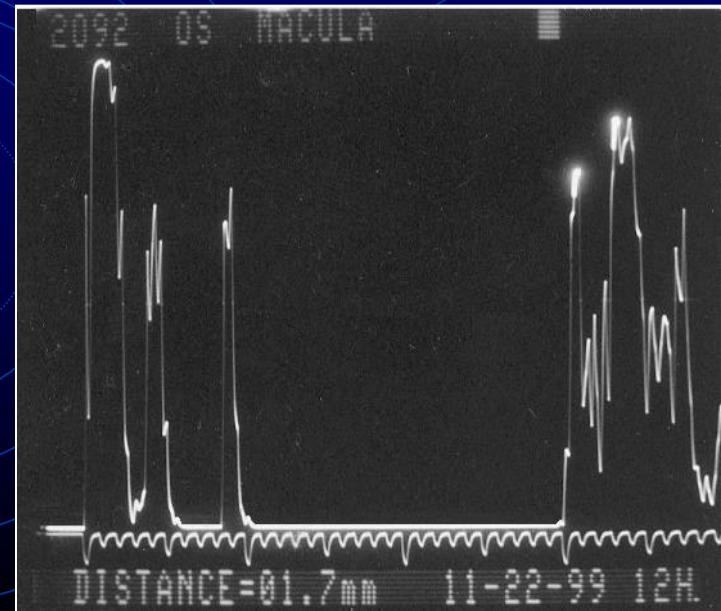
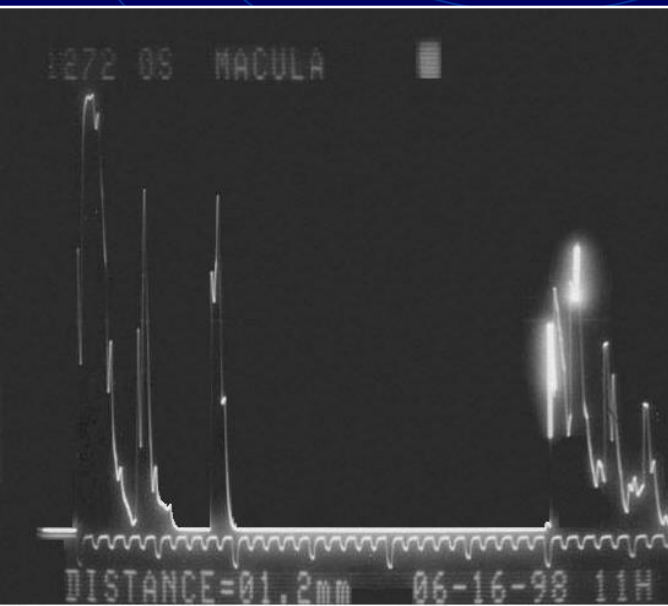
ABSTRACT. At an early clinical stage, patients with cystoid macular oedema show no significant changes in their vision. This phase is described as angiographic cystoid macular oedema. Echographic macular studies have in the past years shown that the macular thickness is increased in the early stages of cystoid macular oedema. In these patients there was no evidence of cystoid macular oedema with the visual acuity test, B-scan echography and fluorescein angiography. In this paper an echographic macular study by standardized A-scan echography was performed in 537 patients before extracapsular cataract extraction and intraocular lens implantation in posterior chamber (ciliary sulcus). The results showed that this method is very sensitive in detecting patients with high risk of cystoid macular oedema.

Key words: cystoid macular oedema - standardized echography - cataract extraction - macular thickness.

Acta Ophthalmol. Scand. 1996; 74: 178-181

Macula normale
≤ 1.5 mm

Macula ispessita



Bianciotto C, Shields CL, Guzman JM, Romanelli-Gobbi M, Mazzuca D Jr, Green WR, Shields JA. Assessment of anterior segment tumors with ultrasound biomicroscopy versus anterior segment optical coherence tomography in 200 cases. *Ophthalmology*. 2011 Jul;118(7):1297-302.

Hau SC, Papastefanou V, Shah S, Sahoo MS, Restori M, Cohen V. Evaluation of iris and iridociliary body lesions with anterior segment optical coherence tomography versus ultrasound B-scan. *Br J Ophthalmol*. 2015 Jan;99(1):81-6

Krema H, Santiago RA, Gonzalez JE, Pavlin CJ. Spectral-domain optical coherence tomography versus ultrasound biomicroscopy for imaging of nonpigmented iris tumors. *Am J Ophthalmol*. 2013 Oct;156(4):806-12.

Merchant KY, Su D, Park SC, Qayum S, Banik R, Liebmann JM, Ritch R. Enhanced depth imaging optical coherence tomography of optic nerve head drusen. *Ophthalmology*. 2013 Jul;120(7):1409-14.

Shields CL, Arepalli S, Atalay HT, Ferenczy SR, Fulco E, Shields JA. Choroidal osteoma shows bone lamella and vascular channels on enhanced depth imaging optical coherence tomography in 15 eyes. *Retina*. 2015 Apr;35(4):750-7.

Evaluation of iris and iridociliary body lesions with anterior segment optical coherence tomography versus ultrasound B-scan.

Hau SC¹, Papastefanou V², Shah S¹, Sagoo MS³, Restori M¹, Cohen V².

RESULTS: The three most common diagnoses were iris naevi (62 (49.2%)), iris pigment epithelial cysts (23 (18.3%)) and iris melanoma (11 (8.7%)). Image feature comparison for USB was better than AS-OCT in visualising all tumour margins (81 (64.3%) vs 59 (46.8%)), posterior tumour margin (54 (42.9%) vs 16 (12.7%)) and producing less posterior shadowing (121 (96%) vs 43 (34.1%)). Image resolution comparison revealed USB to be slightly better for resolving the overall tumour (45 (35.7%) vs 43 (34.1%)) and posterior tumour surface (70 (55.6%) vs 32 (25.4%)) but AS-OCT was better for resolving the anterior (62 (49.2%) vs 4 (3.2%)) and lateral tumour surface (62 (49.2%) vs 31 (24.6%)). Comparing the three most common diagnoses, USB was better for visualising iris pigment epithelial cysts (12 (52.2%) vs 2 (8.7%)) and iris melanoma (7 (63.6%) vs 1 (9.1%)) but AS-OCT was better (28 (45.2%) vs 15 (24.2%)) for visualising iris naevi. Bland-Altman plots showed good agreement between the two techniques for lesions smaller than 3 mm in base and 2 mm in elevation.

CONCLUSIONS: AS-OCT is superior to USB for imaging small lesions pertaining to the anterior iris but USB is better for imaging larger iris lesions with posterior or ciliary body extension.

Assessment of anterior segment tumors with ultrasound biomicroscopy versus anterior segment optical coherence tomography in 200 cases.

Bianciotto C¹, Shields CL, Guzman JM, Romanelli-Gobbi M, Mazzuca D Jr, Green WR, Shields JA.

RESULTS: There were 200 eyes with anterior segment tumors involving the iris stroma in 96 (48%), ciliary body in 14 (7%), combined iris and ciliary body in 32 (16%), iris pigment epithelium (IPE) in 44 (22%), conjunctiva in 6 (3%), sclera in 4 (2%), and others in 6 (1% each). The diagnoses included nevus in 75 eyes (38%), melanoma in 47 (24%), cyst in 48 (24%), epithelioma (adenoma) in 5 (3%), metastasis, melanocytosis and melanocytoma in 4 eyes each (2%), and others (1% each). Image analysis (UBM vs AS-OCT) revealed adequate visualization of all tumor margins (189 [95%] vs 80 [40%]), posterior tumor shadowing (9 [5%] vs 144 [72%]), and high overall image quality (159 [80%] vs 136 [68%]). Comparison for better image resolution (UBM vs AS-OCT) disclosed UBM provided better overall tumor visualization (138 [69%] vs 62 [31%]) and better resolution of the posterior margin (147 [74%] vs 53 [27%]), whereas AS-OCT provided better resolution of the anterior margin (40 [20%] vs 160 [80%]) as well as better overall resolution of anterior segment anatomy (41 [21%] vs 159 [80%]). Better resolution was found with UBM for pigmented tumors (n = 162; 107 [66%] vs 55 [34%]) as well as for nonpigmented tumors (n = 38; 23 [61%] vs 15 [39%]). Regarding location, iris tumor resolution was similar with each technique (49 [52%] vs 45 [48%]).

CONCLUSIONS: For anterior segment tumors, UBM offers better visualization of the posterior margin and provides overall better images for entire tumor configuration compared with AS-OCT.

Spectral-domain optical coherence tomography versus ultrasound biomicroscopy for imaging of nonpigmented iris tumors.

Krema H¹, Santiago RA, Gonzalez JE, Pavlin CJ.

RESULTS: Thirty-seven patients with nonpigmented iris tumors were included. Comparing SDOCT to UBM, the image definitions of anterior tumor surface and internal tumor heterogeneity were equivalent. Posterior tumor surface was well defined in 54% of SDOCT vs 100% in UBM images. Full tumor thickness measurement was possible in 86% of SDOCT vs 100% with UBM. The maximum measurable tumor thickness with SDOCT was 1.34 mm. SDOCT images showed optical aberrations such as shadowing and ghost images in 22 tumors (59%), which encroached on the tumor image in 8 patients (22%). The overall tumor visualization with SDOCT was possible in 65% of the iris tumors.

CONCLUSIONS: UBM generally provides superior imaging quality and reproducible measurements of nonpigmented iris tumors. Nevertheless, SDOCT, being a noncontact technique, can be a reliable alternative in imaging and following some selected nonpigmented iris tumors.

Enhanced depth imaging optical coherence tomography of optic nerve head drusen.

Merchant KY¹, Su D, Park SC, Qayum S, Banik R, Liebmann JM, Ritch R.

RESULTS: Sixty-eight eyes were clinically classified into 3 groups: 32 eyes with definite ONHD, 25 eyes with suspected ONHD, and 11 normal-appearing fellow eyes. In the definite ONHD group, EDI OCT, non-EDI OCT, and ultrasound B-scan were positive for ONHD in all eyes and visual field (VF) was abnormal in 24 eyes. In the suspected ONHD group, EDI OCT, non-EDI OCT, ultrasound B-scan, and VF were positive in 17, 14, 7, and 3 eyes, respectively; 8 eyes had no evidence of ONHD in any of the tests. In normal-appearing fellow eyes, EDI OCT, non-EDI OCT, ultrasound B-scan, and VF were positive in 3, 1, 1, and 0 eyes, respectively; 4 eyes had no evidence of ONHD in any of the tests. Enhanced depth imaging OCT had a significantly higher ONHD detection rate than ultrasound B-scan in all eyes (52/68 eyes vs. 40/68 eyes; $P < 0.001$), in eyes with clinically suspected ONHD or normal-appearing fellow eyes (20/36 eyes vs. 8/36 eyes; $P < 0.001$), and in eyes with clinically suspected ONHD (17/25 eyes vs. 7/25 eyes; $P = 0.002$). Enhanced depth imaging OCT-detected ONHD appeared as signal-poor regions surrounded by short, hyper-reflective bands or isolated/clustered hyper-reflective bands without a signal-poor core. In non-EDI OCT, posterior surfaces of the ONHD and deep-seated hyper-reflective bands were invisible or less clear than in EDI OCT.

CONCLUSIONS: Enhanced depth imaging OCT detects lesions likely representing ONHD more often and better assesses their shape and structure than conventional tests.

Choroidal osteoma shows bone lamella and vascular channels on enhanced depth imaging optical coherence tomography in 15 eyes.

Shields CL¹, Arepalli S, Atalay HT, Ferenczy SR, Fulco E, Shields JA.

RESULTS: The mean age at presentation was 27 years. There were 10 women and 3 men. The visual acuity ranged from 20/20 to hand motion, with reduced visual acuity secondary to photoreceptor loss in the foveola (n = 5) or subfoveal fluid (n = 1), and additional choroidal neovascular membrane (n = 3). The mean basal tumor diameter was 8.0 mm, and ultrasonographic thickness was 1.5 mm. Using enhanced depth imaging optical coherence tomography, the mean tumor thickness was 589 μm when compared with a matched choroidal region in the unaffected eye of 247 μm (138% increased thickness) ($P = 0.009$). The tumor surface topography was classified (ultrasonography vs. enhanced depth imaging optical coherence tomography) as flat (87 vs. 13%), dome (13 vs. 40%), or undulating (0 vs. 47%). On enhanced depth imaging optical coherence tomography, unique features included horizontal lamellar lines (presumed bone lamella) (n = 15, 100%) and hyperreflective horizontal lines (presumed cement lines) (n = 8, 53%). Other features included horizontal tubular lamella with optically empty center (presumed Haversian canals or vascular channels) (n = 9, 60%), vertical tubular lamella (presumed Volkmann canals or vascular channels) (n = 2, 13%), and speckled regions (presumed compact or small trabecular bone) (n = 6, 40%). Of the nine eyes with subfoveal osteoma, the tumor was completely ossified (n = 4), partially deossified (n = 2), or completely deossified (n = 3). Photoreceptor thinning/atrophy was found in all five eyes with deossified osteoma, whereas intact photoreceptor appearance was noted in the four eyes with ossified subfoveal osteoma.

CONCLUSION: Enhanced depth imaging optical coherence tomography reveals characteristic surface topography of choroidal osteoma as dome or undulating (87%) with unique intrinsic features of horizontal lamellar lines (100%), horizontal (60%) or vertical (13%) tubules, and speckled regions (40%). Photoreceptor loss was evident in every case of tumor deossification.

TAKE HOME MESSAGE

Mezzi diottrici trasparenti

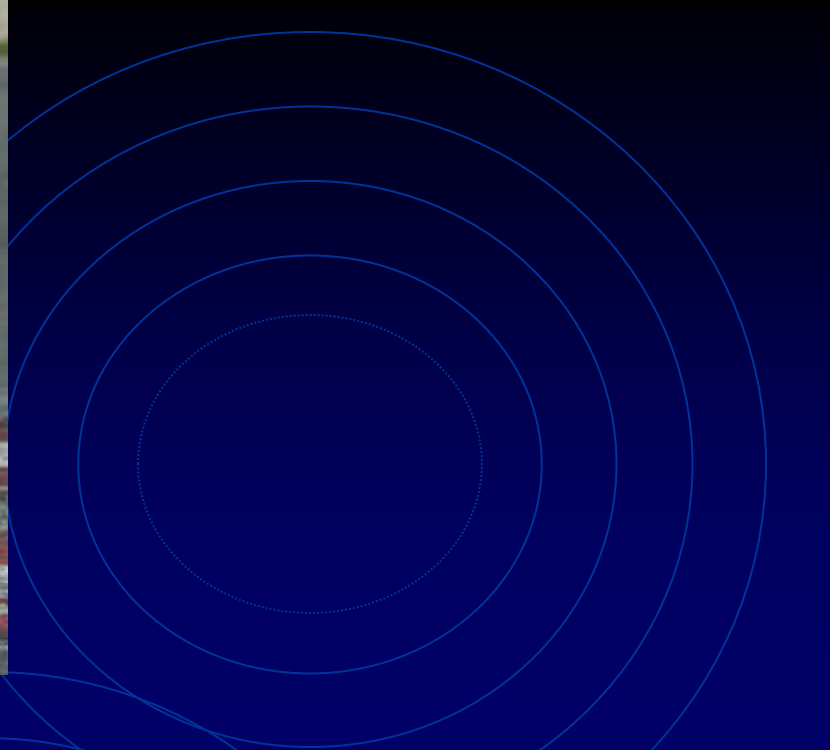
	Neoformazioni	Distacco di retina	Lacerazioni	Maculopatie	Segmento anteriore
ECOGRAFIA	+	+	+	-	+/-
OCT	+/-	+/-	+/-	++	+/-

Mezzi diottrici opachi

	Neoformazioni	Distacco di retina	Lacerazioni	Maculopatie	Segmento anteriore
ECOGRAFIA	+	+	+	+/-	+
OCT	-	-	-	-	-

The background of the slide is a dark blue color. It features several sets of concentric circles in a lighter blue shade, arranged in a pattern that resembles a Venn diagram or a series of overlapping ripples. The circles are centered around the text.

L'OCT ha diminuito le
indicazioni dell'ecografia?



GRAZIE PER L'ATTENZIONE

